

# Emulsion Copolymerization of Tetrafluoroethylene with $\omega$ -Chlorotetrafluoroethyltrifluorovinyl Ether and the Synthesized Copolymer Properties

S. R. Allayarov,<sup>1,2</sup> A. N. Ilyin,<sup>3</sup> Yu. A. Olkhov,<sup>1</sup> U. Yu. Allayarova,<sup>1</sup> D. A. Dixon<sup>2</sup>

<sup>1</sup>*Institute of Problems of Chemical Physics of the Russian Academy of Sciences, Chernogolovka, Moscow, Russia 142432*

<sup>2</sup>*Department of Chemistry, The University of Alabama, Tuscaloosa, Alabama 35487-0336*

<sup>3</sup>*JSC Halogen, Perm, Russia 614113*

Received 4 March 2010; accepted 22 November 2010

DOI 10.1002/app.33808

Published online 21 March 2011 in Wiley Online Library (wileyonlinelibrary.com).

**ABSTRACT:** Emulsion copolymerization of  $\omega$ -chlorotetrafluoroethyltrifluorovinyl ether ( $\text{Cl}(\text{CF}_2)_2\text{OCF}=\text{CF}_2$  (FVE)) with tetrafluoroethylene ( $\text{CF}_2=\text{CF}_2$  (TFE)) was investigated at various monomer ratios. The copolymerization rate is below the rate of TFE homopolymerization and the copolymerization kinetics depends on the FVE content in the reaction medium. The copolymer composition is very similar if the FVE content in monomer mixture is  $\leq 2.5$  mol %. However, the percent amount of FVE in the copolymer, the copolymerization rate, and molecular mass of synthesized copolymers decrease noticeably with increase in the FVE content in the monomer mixture. The constants of copolymerization are  $r_1 = 2.8$  (TFE) and  $r_2 = 0.03$  (FVE). The copolymer is a statistical polymer consisting of TFE blocks and individual FVE molecules between the blocks. The average molecular mass of copolymers is significantly less than that of the TFE homopolymer (PTFE) synthesized at the same conditions. The morphologies of PTFE and copolymer

powders were investigated by thermomechanical analysis and are not similar. The copolymer has a completely amorphous diblock morphology depending on the FVE content. The introduction of FVE molecules into the copolymer macromolecules is accompanied by reduction of the crystalline portion of copolymer. If the FVE content in copolymer is  $\geq 3.5$  mol %, the copolymer macromolecules completely lose the ability to form crystalline portions as a result of their amorphicity. The introduction of up to 2.4 mol % FVE into the copolymer macromolecules yields a highly thermostable and melttable copolymer which can be processed by using the industrial processes used widely for thermoplastics. © 2011 Wiley Periodicals, Inc. *J Appl Polym Sci* 121: 2489–2499, 2011

**Key words:** tetrafluoroethylene;  $\omega$ -chlorotetrafluoroethyltrifluorovinyl ether; homopolymerization; copolymerization; polytetrafluoroethylene; thermomechanical analysis; molecular and topological structure

## INTRODUCTION

Polytetrafluoroethylene (PTFE) is a material with many important applications because of its unique properties, for example, it has the highest chemical and thermal stability among synthetic polymers. However, it is not soluble and a viscous-fluid state of PTFE cannot be obtained, so it cannot be processed into products by using any of the processing methods usually employed for thermoplastics. As a result, the manufacturing techniques of products from PTFE can be very complicated.<sup>1–5</sup> The industrial processes for the production of PTFE can lead

to a substantial amount of waste. Therefore, there is a search for thermoplastic copolymers to replace PTFE. Such copolymers should possess the same unique properties as PTFE, but they should be processable by methods used for the manufacture of typical thermoplastic polymers. The replacement of PTFE with copolymers of TFE and perfluoroalkylvinyl ether (PFAVE) is one such example.<sup>6–8</sup>

The mechanism of polymerization and copolymerization of PFAVE molecules has not been extensively studied. The influence of PFAVE molecules on their ability to copolymerize with TFE was investigated.<sup>7</sup> Because of the operational constraints of the Alfrey-Price scheme,<sup>9</sup> the previous study<sup>7</sup> could not establish a relationship between the structure and reactivity of the PFAVE molecules. The prior study<sup>7</sup> showed that lengthening the perfluoroalkoxyl fragment of the PFAVE molecules results in an appreciable decrease in their reactivity in copolymerization with TFE.

Polymerization and copolymerization of branched perfluoroolefins often do not obey the classical kinetics for a chain process. This behavior differs from

Correspondence to: D. A. Dixon (dadixon@bama.ua.edu).

Contract grant sponsor: US Civilian Research and Development Foundation; contract grant number: RUC2-2287-CG-06.

Contract grant sponsor: Robert Ramsay Fund at The University of Alabama.

the behavior of their hydrocarbon analogs. For example, substitution of a fluorine atom by a trifluoromethyl group in the TFE monomer to generate hexafluoropropylene (HFP) stops the chain mechanism for HFP homopolymerization; TFE homopolymerizes<sup>6</sup> at a high rate, but, HFP does not polymerize under similar conditions.<sup>10,11</sup> The polymerization of the hydrocarbon analog of HFP, propylene, occurs by a chain mechanism and, unlike HFP, propylene polymerizes with the same high rates as ethylene. HFP has a low reactivity in copolymerization as well. At high concentrations of HFP in the reaction zone, the chain process can be completely suppressed. Therefore, the HFP content in current industrial perfluorocopolymers cannot exceed 20 mol %.<sup>11</sup> Various mechanisms have been proposed to explain the chain polymerization of HFP as a comonomer.<sup>11</sup> Some assume that it may be connected with the electrostatic properties of the trifluoromethyl groups, which decrease the reactivity of the C=C double bonds. Others explain the low reactivity of HFP in terms of a steric shielding of the C=C double bond by the trifluoromethyl group, which can interfere with the ability of another HFP molecule to reach the reaction center. The behavior of HFP in radical polymerization has been also explained by the formation of a long lived liquid radical (LLR) at some stage of HFP oligomerization.<sup>11</sup> Such LLRs terminate the propagating chain and are not capable of mutual recombination. As a result, the homopolymerization or copolymerization of HFP is terminated if LLRs are formed. The validity of this hypothesis has been demonstrated in the polymerization of TFE in the presence of perfluoroolefins, such as HFP, the HFP dimer ((HFP)<sub>2</sub>), and the HFP trimer ((HFP)<sub>3</sub>). HFP and (HFP)<sub>2</sub> show an ability to effectively trap the active propagating radicals. However, (HFP)<sub>3</sub> as well as linear perfluoroalkanes do not participate in polymerization as a terminator because their molecules are not able to react with the propagating radicals. (HFP)<sub>3</sub> can react only with an atomic fluorine and not with any larger radicals.<sup>12</sup> Therefore, (HFP)<sub>3</sub> is practically an inert solvent and TFE polymerization occurs in it with practically the same rate as for the homopolymerization of pure TFE. It can be assumed that branched perfluoroolefins, such as PFAVEs, should behave like HFP in radical chain processes. However, the nature of the low reactive propagation radical formation has been considered only in the case of the TFE homopolymerization in presence of HFP or its oligomers.<sup>11</sup>

The molecular mass (MM) and molecular mass distribution (MMD) of the copolymer product can help to elucidate the copolymerization mechanism. Information about the dependence of the MM on the content of comonomers allows us to investigate the low reactivity due to the formation of LLRs. The MM together with the chemical composition of the macromolecule defines the physical, chemical, and mechan-

ical properties of the copolymers. An important characteristic of fluoro-containing copolymers and polymers are their topological structure,<sup>13,14</sup> including the macromolecular structure (linear, crosslinked, branched) and the interchain behavior (temperature of transitions, linear thermal expansion, free volume). For many copolymers, the important molecular and topological parameters can be measured by the classical methods of polymer structural analysis, such as DSC, X-ray, NMR, etc. The MM and MMD can be determined by gel permeation chromatography.<sup>15</sup> Other methods for determining the polymer molecular heterogeneity are based on the use of dilute solutions of linear polymers, and the measurement of the swelling process of the crosslinked structure of the polymers. The perfluorinated copolymers of interest in this study, however, are not easily dissolved. Therefore, their macromolecular parameters need to be determined by using indirect methods based on the heat treatment of the samples.<sup>8,9</sup> However, this leads to the thermal destruction of the polymer, which decreases the MM and changes the topological structure of the polymer.

Thermomechanical spectroscopy (TMS) is a novel solid-phase diagnostic tool for studying polymers and allows complex molecular topological testing of the polymers. An example of the effective use of the TMS method to investigate the molecular and topological structure of fluorine containing polymers is a study of polyvinylidene fluoride and the copolymer of TFE with ethylene.<sup>13</sup> Recently, the TMS method was applied to the quantitative analysis of effect of radiation on molecular and topological structure of PTFE.<sup>14</sup> The present work is a study of the kinetics of copolymerization of TFE with FVE and of the molecular topological structure and thermostability of the synthesized copolymer.

## EXPERIMENTAL

Tetrafluoroethylene was obtained from "JSC 'Halogen'" (starting purity 99.9%). The basic impurities in TFE were difluoromethane and trifluoromethane. The sum of their contents were  $1.2 \times 10^{-2}\%$ . Triethylamine was the inhibitor in TFE instead of "limonene." The TFE was purified from triethylamine by filtration through absorbent coal and a 20% solution of sulfuric acid. The  $\omega$ -chlorotetrafluoroethyltrifluorovinyl ether  $\text{Cl-CF}^1\text{F}^1\text{-CF}^2\text{F}^2\text{-O-CF}^5 = \text{CF}^4\text{F}^3$  (FVE) was synthesized using the method described previously.<sup>16</sup> The synthesized FVE has  $T_b = 37^\circ\text{C}$  and  $d_4^{20} = 1.645$ . In the NMR <sup>19</sup>F spectra of FVE, there are: 1–2.7 ppm;  $J_{(2-4)} = 6.1$  Hz; 2–12.7 ppm;  $J_{(2-1)} = 2.0$  Hz; 3–39.3 ppm;  $J_{(5-4)} = 112$  Hz; 4–46.7 ppm;  $J_{(5-3)} = 66$  Hz;  $J_{(4-3)} = 86$  Hz; 5–59.6 ppm, and  $J_{(5-1)} = 1$  Hz. In the synthesized FVE, the amount of basic product is 99.8%. The ratio of the

amount of elements in the FVE determined by elemental analysis and calculated from the NMR data are: 20.40/20.69 (C); 14.85/15.09 (Cl), and 56.95/57.33 (F). The water was triply distilled. The emulsifier and initiator were, respectively, ammonium perfluorooxononanoate ( $C_8F_{17}CO_2NH_4$ , 98.4%) and the succinic acid peroxide (99.1%) obtained from JSC Halogen. These chemicals used were reagent grade. The temperature of polymerization was 70–75°C.

The pressure for polymerization was maintained at  $22 \pm 0.5$  atm. The temperature of polymerization was 70–75°C and was chosen from an analysis of literature data and our own experience. Emulsion polymerization of TFE and other fluorinated monomers is usually carried out at these temperatures when using succinic acid peroxide as the initiator. Thus, we considered the temperature of polymerization to be  $72.5^\circ C \pm 2.5^\circ C$ . Stirring was done at a rate of  $670 \text{ turns min}^{-1}$ .

The copolymerization product was a white dispersion in water. It was coagulated using HCl and washed up to neutral pH using distilled water. Afterward, it was washed with ethanol to remove the emulsifier. Then, the product was dried to a constant mass in a vacuum system. The FVE content in the copolymer was determined by elemental analysis. Conversion of TFE and FVE has been measured gravimetrically and by measurement of the TFE pressure in the reactor.

$M_1$  and  $M_2$  are the TFE and FVE content in the monomer mixture, respectively;  $m_1$  and  $m_2$  are the TFE and FVE molar content in the copolymer, respectively.  $M_1 + M_2 = m_1 + m_2 = 100 \text{ mol } \%$ . The initial FVE content in the monomer mixture in reactor was varied from 1.0 mol % up to 20 mol % (see the summary listing of symbols). The color of the copolymers of TFE with FVE is white and does not differ from the color of the PTFE synthesized under comparable experimental conditions.

Thermomechanical analysis of the polymeric products was carried out by insertion of a quartz hemispherical probe into the polymer. The dynamics of the interaction of the probe with a polymer surface has been described.<sup>17</sup> The tested polymer samples had two plane-parallel sides separated by tens of mm. One of the measured values is a change in the linear size of a sample between a substrate and the probe. The polymer powder of 0.2–1.0 g was compressed at room temperature under an optimized pressure of 190–250 atm using a DP36 press from Carl Zeiss Jena. The diameter of the metallic form used for pressing is 6 mm and meets the #14 Russian standards for surface treatment. The resulting pellet was placed in the chamber of a UIP-70M thermoanalyzer and cooled to  $-100^\circ C$  at a rate of  $5^\circ \text{ min}^{-1}$ . It was maintained at this temperature for 5 min and then the probe loaded with a force of 0.5 g. The sample was then heated at a rate of

$5^\circ \text{ min}^{-1}$ . A summary of the TMS investigation of fluoro-containing polymers has been described previously.<sup>13</sup> The TMS method is based on measurements of sample deformation under a very low load in the thermal field which is time-dependent [the thermomechanical curve (TMC)] leading to measurements of the glass transition temperature and the temperature for the beginning of molecular flow. The methodology of the measurements and calculations of MMD, including the determination of the amount of different blocks, and related characteristics have been described in detail.<sup>18–24</sup> The accuracy and reproducibility of the TMS method has been described previously.<sup>25</sup> The use of the TMS method for fluoropolymers, particularly PTFE, has been discussed in detail.<sup>13,26</sup> The accuracy of the temperature measurements in the thermostatic chamber of the instrument is  $\pm 0.05^\circ C$ . The accuracy of the deformation measurement is  $\pm 5 \text{ nm}$ . The errors of MM and free volume fraction are  $\leq \pm 10\%$ . The data were reproducible, in general to within error limits of  $\pm 5\text{--}10\%$ , but in some cases, these errors can be as large as  $\pm 20\%$  due to the heterogeneity of the materials and differences in their thermal and stress history. The thermostability of the polymer products were determined by using standard differential thermal analysis on the derivatograph KU-200.

## RESULTS AND DISCUSSION

### Kinetics of TFE homopolymerization and its copolymerization with FVE

The kinetics of TFE homopolymerization results in an S-type curve, which is typical for emulsion polymerization (Fig. 1, Curve 1). The polymerization has an induction period and after 20–30 min, it reaches a constant rate, which continues up to 70% conversion of the TFE. In Figure 2, the lower curve shows the TFE conversion after 90 min of polymerization, and, in this case, the conversion is 50% when  $M_2 = 0$ . According to Curve 1, Figure 1, if the time for TFE homopolymerization is increased to 130 min, the conversion reaches 70%. After this point, the rate of polymerization decreases and it takes up to 280 min for the conversion of TFE to reach 90%. The rate of the chain propagation stage of TFE homopolymerization is very high due to the reactive  $C=C$  bond in TFE and there is only a small energy of activation.<sup>6</sup> For the majority of monomers except TFE, the chain termination steps occur with a small energy of activation and hence a high rate. However, for TFE homopolymerization, the chain termination occurs with a low rate due to the properties of the propagating radicals, which leads to the formation of long propagating chains, so the final PTFE has a very high molecular mass. The average molecular mass of

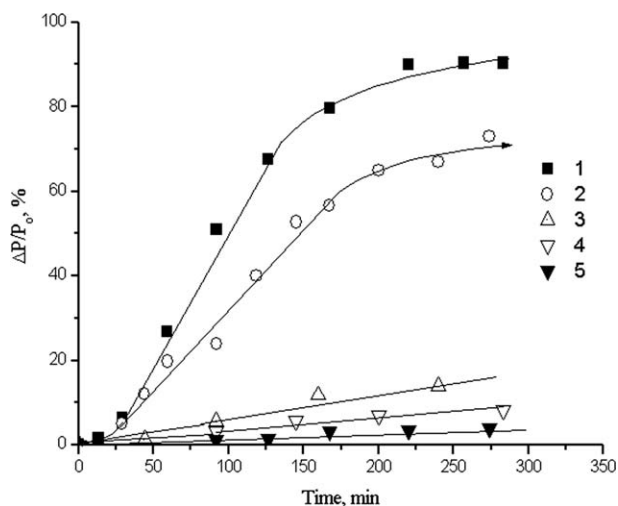


**Figure 1** Time-conversion curve of TFE homopolymerization (1) and the TFE copolymerization with FVE (2–5). The FVE content in monomer mixture was 1.0–2.5 mol % (2), 5.0 mol % (3), 12.5 mol % (4), and 20 mol % (5). The average deviation of values of TFE conversion is  $\pm 2\%$  (1,3,4,5) and  $\pm 5\%$  (2).

the topological regions of the synthesized PTFE determined by the TMS method is  $22.56 \times 10^6$ . The values of the MM in Table I are similar to the MM of commercial PTFE powders analyzed by TMS.

As shown in Figure 1, the rate of copolymerization of TFE with FVE (Curves 2–5) is below that of TFE homopolymerization (Curve 1). The kinetics of copolymerization also exhibit an S-type curve (Curve 2), as found for TFE homopolymerization if the initial mixture of monomers contains  $\leq 2.5$  mol % of FVE. In such samples, a constant rate of copolymerization is established after 20–30 min. After conversion of 60% of the TFE, the copolymerization essentially stops.

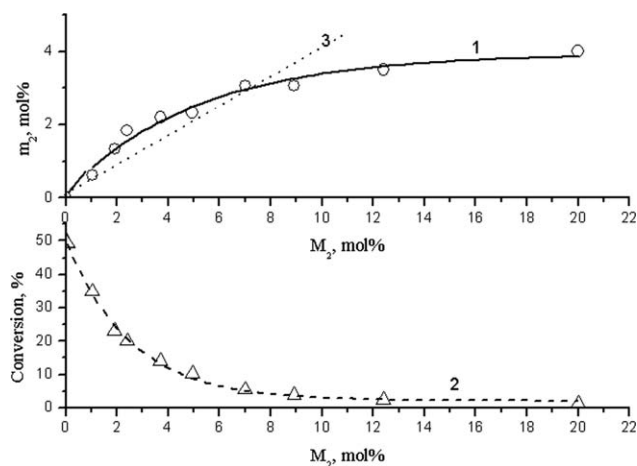


**Figure 2** The FVE content in copolymer ( $m_2$ ) (1) and conversion of TFE (2) as a function of the FVE content ( $M_2$ ) in initial mixture of TFE and FVE. Plot of calculated composition of copolymer (3) for values  $r_1 = 2.8$  and  $r_2 = 0.03$ .

**TABLE I**  
Molecular and Topological Structures  
of the PTFE Powder

| Parameters                                  | Co-axial orientation of vectors | Perpendicular orientation of vectors |
|---|---------------------------------|--------------------------------------|
| Amorphous region                            |                                 |                                      |
| $T_{g'}^{\circ}\text{C}$                    | 17                              | 17                                   |
| $\alpha_1 \cdot 10^5 \text{ deg}^{-1}$      | 9.16                            | 9.26                                 |
| $\alpha_2 \cdot 10^5 \text{ deg}^{-1}$      | 49.0                            | 33.9                                 |
| $V_f$                                       | 0.347                           | 0.214                                |
| $\overline{M}_{g_n} \cdot 10^{-3}$          | 466.1                           | 687.2                                |
| $\overline{M}_{g_w} \cdot 10^{-3}$          | 849.6                           | 1217.8                               |
| $K_a$                                       | 1.82                            | 1.77                                 |
| $\varphi_a$                                 | 0.50                            | 0.58                                 |
| Low-melting crystalline portion             |                                 |                                      |
| $T_{m'}^{\circ}\text{C}$                    | 327                             | 327                                  |
| $\alpha_k \cdot 10^5 \text{ deg}^{-1}$      | 357.1                           | 358.2                                |
| $\overline{M}_n^{cr1} \cdot 10^{-3}$        | 15.8                            | 39.8                                 |
| $\varphi_{cr}$                              | 0.37                            | 0.12                                 |
| High-melting crystalline portion            |                                 |                                      |
| $T_{m''}^{\circ}\text{C}$                   | 347                             |                                      |
| $\alpha'_k \times 10^5 \text{ deg}^{-1}$    | 64.1                            |                                      |
| $\overline{M}_n^{cr2} \cdot 10^{-6}$        | 74.54                           |                                      |
| $\overline{M}_w^{cr2} \cdot 10^{-6}$        | 77.22                           |                                      |
| $K''_{cr}$                                  | 1.04                            |                                      |
| $\varphi''_{cr}$                            | 0.13                            | 0.0                                  |
| High-temperature amorphous (cluster) region |                                 |                                      |
| $T_{cl}^{\circ}\text{C}$                    |                                 | 353                                  |
| $\alpha_{cl} \times 10^5 \text{ deg}^{-1}$  |                                 | 34.2                                 |
| $(M_{(n)cl} \times 10^{-6})$                |                                 | 68.74                                |
| $(M_{(w)cl} \times 10^{-6})$                |                                 | 72.87                                |
| $K_{cl}$                                    |                                 | 1.06                                 |
| $\varphi_{cl}$                              | 0.0                             | 0.30                                 |
| $T_{f'}^{\circ}\text{C}$                    | 465                             | 465                                  |
| Values averaged between regions             |                                 |                                      |
| $\overline{M}_w \cdot 10^{-6}$              | 10.47                           | 22.56                                |
| $K_{an}$                                    | 0.8                             |                                      |

The FVE content in the copolymer as a function its content in initial monomers mixture is plotted of in Figure 2, Curve 1. The composition of copolymer is very similar to the initial ratio of monomers when the FVE content in the reactants is  $\leq 2.5$  mol %. The fraction of FVE incorporated into the copolymer decreases with increasing the ratio of FVE in the reactants from 3 to 5 mol %. When the FVE content in the reactants is 7–20 mol %, the FVE content in the copolymer does not exceed 3–4 mol %. When the FVE content in the initial mixture of comonomers is more than 5 mol %, the TFE conversion does not exceed 10% (Fig. 2, Curve 2). In such cases, according Figure 2, Curve 1, the FVE conversion does not exceed 50%.

The dependence of TFE conversion on the FVE content in the comonomer mixture is presented in Figure 2, Curve 2. Comparing Curves 1 and 2 in Figure 2, the decrease in TFE conversion is shown to be accompanied by an increase of the content of the FVE molecules in the copolymer product. When the FVE content in initial mixture of comonomers is

more than 5 mol %, the TFE conversion does not exceed 10%. In such cases, there is a decrease of the copolymerization rate (Fig. 1) and of the amount of TFE conversion (Fig. 2, Curve 2) due to a loss of highly reactive TFE molecules in the reaction medium. The FVE monomers are responsible for these changes. If the mixture of TFE and FVE has an FVE content  $\geq 20$  mol %, then the chain propagation of copolymerization is essentially terminated (Fig. 2, Curve 5).

The method described previously<sup>27</sup> was used to define the constants of TFE copolymerization with FVE. The dependence of the composition of the copolymer ( $m_1, m_2$ ) on the composition of the initial mixture ( $M_1, M_2$ ) of TFE ( $M_1, m_1$ ), and FVE ( $M_2, m_2$ ) is presented in Figure 3. The copolymerization constants can be determined from the limit of Curves 1 and 2 in Figure 3 at high levels of the monomer concentrations in the reaction mixture.<sup>27</sup> The resulting constants for the copolymerization of TFE ( $r_1$ ) and FVE ( $r_2$ ) are  $r_1 = 2.8$  and  $r_2 = 0.03$ . In Figure 2, Curve 3 shows the dependence of the copolymer composition calculated using Eq. (1),<sup>28</sup>

$$m_1/m_2 = (r_1 M_1/M_2 + 1) / [(r_2 + M_1/M_2) / (M_1/M_2)] \quad (1)$$

The calculated copolymer compositions (Curve 3) only describe the initial part of the observed copolymer composition curve (Fig. 2, Curve 1). The value of  $r_1 = 2.8$  shows that the synthesized copolymer represents a statistical polymer consisting of blocks of TFE molecules. Analysis of the copolymerization parameters ( $r_1 \times r_2 = 0.084$ ,  $r_1 > 1$ ,  $r_2 \ll 1$ ) shows that the TFE and FVE molecules are alternating in the copolymer and that the propagating radical reacts more readily with TFE than FVE. As a result, the copolymer macromolecules are enriched in TFE and this is especially obvious when the FVE content in the reaction medium is  $> 2.5$  mol % (see Fig. 2, Curve 1). For example, for the case of a molar ratio of comonomers in the reaction mixture of  $M_1/M_2 = 95$ , the ratio in the copolymer is  $m_1/m_2 = 150$ . Thus, in the synthesized copolymer, individual molecules of FVE are included between blocks of TFE molecules.

### The molecular and topological structure of powders of polytetrafluoroethylene and copolymers of TFE with FVE

Investigation of the molecular and topological structure of the polymer powders by the TMS method assumes their one-dimensional compression under optimized pressure. In this case, amorphous-crystal polymers lose their isotropic structures and transform into anisotropic structures. The results show that both the degree of crystallinity and the orientation of the crystals are changed. Some parts of the crystals become oriented perpendicular to the com-

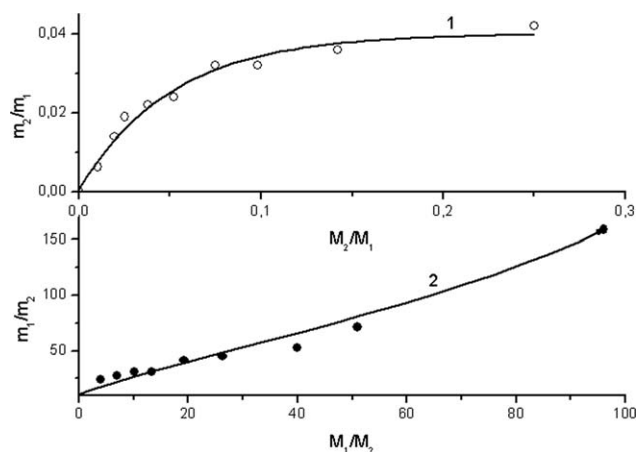


**Figure 3** Dependence of the composition of the copolymer ( $m_1, m_2$ ) from the composition in initial mixture ( $M_1, M_2$ ) of TFE ( $M_1, m_1$ ) and FVE ( $M_2, m_2$ ).

pression pressure vector. Thus, the change of the isotropic polymer structure is one of the most important reasons of structural failure because it causes cracking of cylindrical patterns during their preparation.

The degree of the sample crystallinity can be determined by thermomechanical analysis under two analytical conditions, coaxial (II) and perpendicular ( $\perp$ ).<sup>13,26</sup> The vector of the compression pressure and the vector of loading during the release of the polymer deformation in the thermoanalyzer can be in the same plane (coaxial analysis) or in perpendicular planes. The ratio of the degree of crystallinity determined by these two methods ( $K_{an} = \varphi_{cr(II)}/\varphi_{cr(\perp)}$ ) can be considered as a measure of the structural anisotropy.

Figure 4(a) shows the TMC of the PTFE tested in the coaxial orientation of vectors in the temperature range from  $-100$  to  $500^\circ\text{C}$ . It is characteristic of poly-block amorphous-crystalline PTFE. It contains one amorphous region and two crystalline regions. Parameters of these topological structures are listed in Table I. According to the TMC in Figure 4(a), the lowest relaxation transition (the second kind) of PTFE appears only at room temperature. The relaxation transition at  $123^\circ\text{C}$  reported in Refs. 1–5 has not been confirmed. The glassy temperature of the amorphous fraction is similar to that reported previously.<sup>29</sup>

Expansion of the glassy amorphous PTFE occurs from  $-100^\circ\text{C}$  to room temperature at a constant rate equal to the linear thermal expansion factor  $\alpha_1$  giving a straight line. Thermomechanical (penetrant) deformations of the amorphous fraction of PTFE begin above  $T_g$  as a result of a monotonic decrease of the equilibrium modulus of a pseudonetwork of the amorphous region. The area under the curve of the deformation jumps, which follow a change of the modulus of the network, is a transition area of the amorphous fraction of PTFE. Taking into account the coordinates in which the transition area

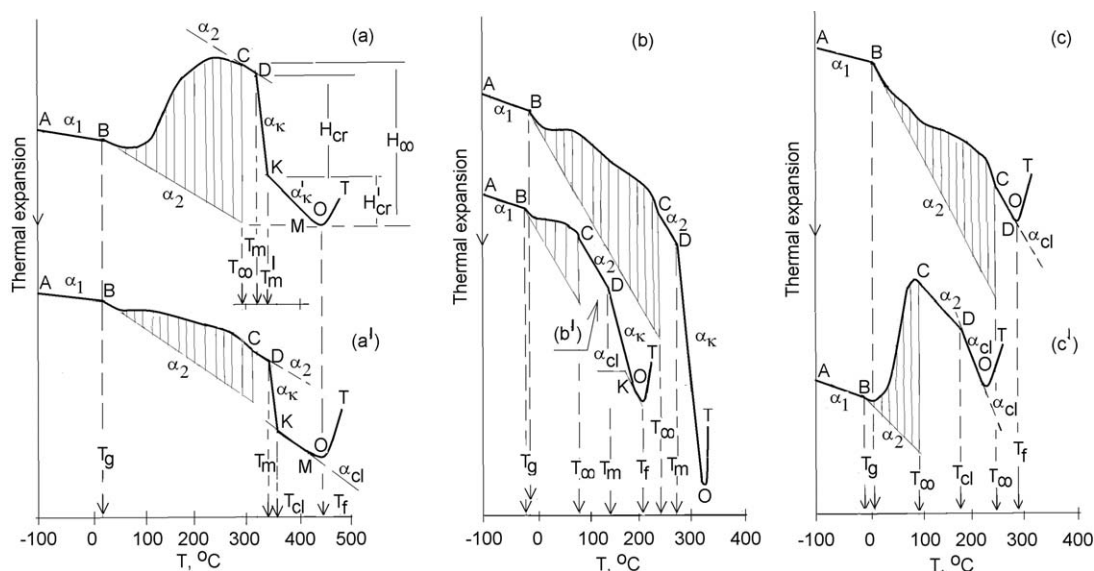


**Figure 4** The TMCs of powders of PTFE (a,a') and the copolymers of TFE with FVE (b,b',c,c'). TMCs were tested in coaxially (a,b,c) and perpendicular (a',b',c') orientation of the vectors. The copolymers were synthesized at the FVE content 2.5 mol % (b,b') and 7 mol % (c,c') in an initial mixture of the monomers.

occurs and using the theory of thermomechanical spectroscopy, this represents a pseudointegrated curve of the MMD of the chain segments between junctions in a pseudonetwork of amorphous region. At the temperature  $T_\infty$ , the chain segment between junctions with the highest molecular mass transforms into a flow or gel-condition. For our samples of PTFE, this state is reached at a temperature of 300°C.

The MM of PTFE homologues is proportional to the magnitude of  $\Delta T = T_\infty - T_g$  and can be determined from Eq. (2).<sup>30</sup>

$$\text{Log } M_{\text{max}} = 2.3 + 11\Delta T / (100 + \Delta T) \quad (2)$$

The MM of PTFE is usually obtained by indirect methods,<sup>6,31</sup> and, in most cases, the measurements are taken after heat treatment, so the less thermostable structures may collapse. Unfortunately, the analysis in the literature<sup>6,31</sup> testifies to the poor agreement of the available data. It is impossible to characterize macromolecules of PTFE by a direct method as the polymer cannot be transferred into soluble or plastic states. Therefore, it is best to discuss and analyze the molecular mass characteristics of PTFE in terms of topological units. Then, the MM may be deduced by unit summation. The MM of the synthesized PTFE as determined by the TMS method has been defined in all its topological units with the data listed in Table I.

At temperatures above  $T_\infty$  as shown by Point C in Figure 4(a), an amorphous fraction of PTFE transitions to a region of high elasticity in which expansion of the polymer with an increase in temperature occurs due to an increase of the free volume of the

polymer  $V_f$ . This region is characterized by the magnitude of the linear thermal expansion factor  $\alpha_2$ . The relation between the glass transition temperature and the values of  $\alpha_1$ ,  $\alpha_2$ , and  $V_f$  is given by Eq. (3).<sup>32</sup>

$$V_f = 3(\alpha_2 - \alpha_1)T_g \quad (3)$$

The values of the calculated free geometrical volume (see Table I) characterize the amorphous region of the synthesized PTFE as a rigid-chain polymer.

The chain segments between junctions in a pseudonetwork of amorphous regions penetrate chain segments in crystallized areas which serve as branch points. Therefore, the heat stability of the chain segments between junctions in a pseudonetwork of the amorphous region is limited to the melting temperature of the crystalline portion (Point D on the TMC curve). Melting of the crystalline portion of the chain segments is indicated by a sharp rate increase in the expansion deformation,  $H_{cr}$ . Melting of the crystalline portion occurs when this factor equals  $\alpha_k$ . It is proportional to the integral specific deformation of expansion ( $H_{cr}/H_0$ ). However, due to the definition of the amount of the crystalline portion, it is necessary to normalize values of  $H_{cr}$  by the thickness of the sample. However, in the case of the amorphous topological region, this normalization is not done. Therefore, in the figures, the ratio of heights  $H_{cr}/H_0$  differs from the amounts of the topological units listed in the tables.

At temperature K, melting of the low-melting crystalline portion is complete and melting of the refractory (other modification) crystalline portion  $T'_m$  begins. The rate of the deformation effect is defined

by the magnitude of the linear thermal expansion factor  $\alpha'_k$  and the fact that  $\alpha'_k/\alpha_1 \geq 6$ . Both crystalline portions become amorphous (simultaneous with melting); then with further temperature increase, segmental relaxation begins. At temperature  $M$ , the thermomechanical deformation of the polymer begins. The deformation is complete at a temperature about  $5^\circ\text{C}$  higher than Point O followed by molecular flow (the curve OT). The temperature of the beginning of molecular flow of PTFE is  $T_f = 465^\circ\text{C}$ . At temperatures above  $470^\circ\text{C}$ , thermal degradation of PTFE macromolecules begins with gas evolution and a loss of mass, as confirmed by thermogravimetric analysis of PTFE (Fig. 5, Curve 1). Curve 1 in Figure 6 is the DTA curve which shows that up to  $327^\circ\text{C}$  (Point A) the polymer is amorphous-crystalline. Above  $327^\circ\text{C}$ , the endothermic melting of the crystalline portion occurs. This process is complete at  $\sim 447^\circ\text{C}$  (Point B) when the polymer becomes completely amorphous.

The exothermic effects occur only at  $515^\circ\text{C}$  (Point C on the differential thermal analysis curve), which can be interpreted as the temperature at the beginning of thermal destruction of covalent bonds in PTFE. The TGA curve, however, shows that the polymer has already lost about 3% of mass before reaching  $515^\circ\text{C}$  (Fig. 5, Curve 1). This is not due to thermal breaking of the C—C or C—F bonds. Curves TGA and DTA show that loss of mass begins at  $470^\circ\text{C}$  and  $5^\circ\text{C}$  above the temperature when molecular flow begins ( $T_f = 465^\circ\text{C}$ ).

The TMC of the PTFE tested in the perpendicular orientation of vectors is presented in Figure 4(a').

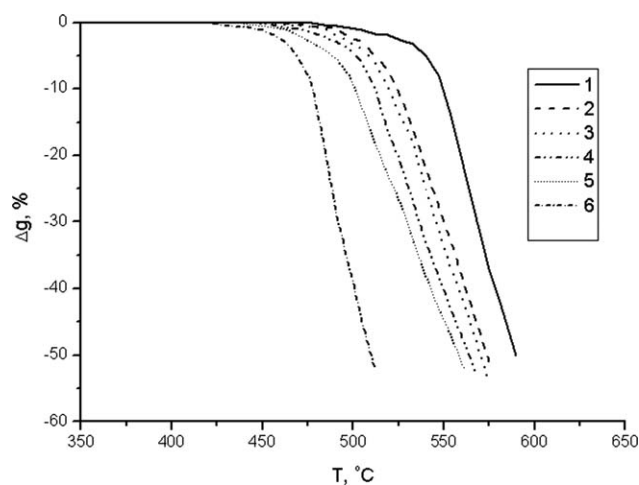


**Figure 5** TGA thermograms for PTFE (1) and the copolymers of TFE with FVE (2,3,4,5). The FVE content in the copolymer (% mole) are 0.71 (2), 1.39 (3), 1.92 (4), 2.4 (5), and 3.5 (6). The molecular masses determined in the coaxial orientation of TMS and averaged between all topological regions are  $10.47 \times 10^6$  (Curve 1),  $53.2 \times 10^3$  (Curve 5) and  $58.4 \times 10^3$  (Curve 6).

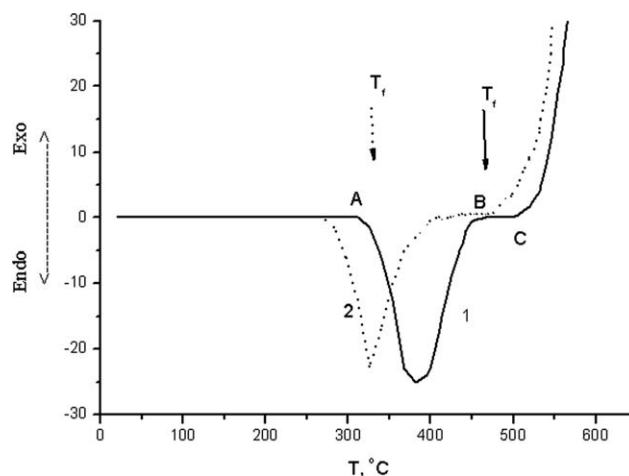


**Figure 6** The curves of DTA analysis of PTFE (1) and the copolymer of TFE with FVE (2). The FVE content in the copolymer is 2.4 mol %. The temperature of the molecular flowing  $T_f$  is tested by the TMS method.

For the perpendicular orientation of the vectors, the phase transitions are practically the same as those of PTFE in the parallel orientation. There is one difference in the TMCs of PTFE measured in the perpendicular and parallel orientations of vectors. The high-temperature amorphous region (cluster) is observed in the perpendicular orientation instead of the high-melting crystalline portion observed in the TMC in the coaxial orientation of vectors. The cluster region measured in the perpendicular orientation of the vectors has the transition temperature  $T_{cl} = 353^\circ\text{C}$ . Parameters of the molecular and topological structures of the perpendicular oriented PTFE are listed in Table I.

The observable difference in average weight molecular mass of blocks ( $\overline{M}_w$ ) in the coaxial and perpendicular orientations of the vectors can be explained by the fact that several crossings of different crystal modifications by macromolecular chains occur in the coaxial orientation. Therefore, the  $\overline{M}_w$  obtained in the perpendicular analysis is closer to the actual value. Molecular flow of the PTFE tested in perpendicular orientation of vectors starts at  $T_f = 465^\circ\text{C}$  as in the coaxial orientation of vectors. Hence, only  $5^\circ\text{C}$  remains between the temperature of flow ( $T_f = 465^\circ\text{C}$ ) and the start of destruction ( $T_d = 470^\circ\text{C}$ ) of the PTFE macromolecules. These characteristics do not allow processes used in processing simple thermoplastic polymers for the manufacture of products from PTFE.

The molecular and topological structure of copolymer of TFE with FVE differs from the structure of PTFE synthesized under the same conditions. As a result of the more regular and dense packing of macromolecules in the crystalline region of PTFE, the effect of including the FVE molecules on its

properties is appreciable. This is manifested by a decrease of crystallized chains in the low temperature crystalline structure of PTFE and by the disappearance of its high melting crystalline region if there is 2.4 mol % of FVE.

The TMC of the copolymer tested in the coaxial orientation of vectors [Fig. 4(c)] is characteristic of a diblock copolymer. There are both amorphous and crystalline regions present. At  $T_m = 290^\circ\text{C}$ , the crystalline portion begins to melt with the rate  $\alpha_k = 205.6 \times 10^{-5} \text{ deg}^{-1}$ . The MM of the crystalline region is proportional to  $\Delta T = T_g - T_m$  and is  $31.6 \times 10^3$ . The amount of the crystalline fraction ( $\phi_k$ ) is proportional to  $H_{cr}$  and is 0.35. At  $-7^\circ\text{C}$ , the segments of chain in the amorphous region transition into the glassy state.

The average numerical and average weight molecular masses in the amorphous region are  $\overline{M}_{gn} = 35.4 \times 10^3$  and  $\overline{M}_{gw} = 64.8 \times 10^3$ , respectively. The value of the average molecular mass of all topological regions is equal to  $\overline{M}_w = 53.2 \times 10^3$ . The molecular mass of the copolymer is  $\sim 200$  times less than the MM of PTFE synthesized under the same conditions (see Tables I and II).

The presence of FVE monomers leads to a deceleration in the growth of the propagating chain for copolymerization and as a result the macromolecular length is shortened leading to a lower molecular mass. It is especially appreciable when a reaction mixture contains more FVE molecules. At a concentration of FVE = 12.5 mol % in the reactants, the MM of the synthesized copolymer is almost a hundred times less than the MM of PTFE synthesized under the same conditions. The amount of FVE in this copolymer is 3.5 mol %. An increase in the amount of FVE monomer in the composition of the copolymer is accompanied by a reduction of the chain segments in crystalline portion of the copolymer. Therefore, the TMC of the copolymer containing 2.4 mol % of FVE does not show a high melting crystalline portion, in contrast to what is observed in the TMC of PTFE. Both the high melting and the low melting crystalline regions observed in the TMC of PTFE disappear completely in the TMC of a copolymer containing 3.5 mol % of FVE. Consequently, the copolymer macromolecules completely lose the ability to form a crystalline structure if they have  $\geq 3.5$  mol %. If there are more than 100 TFE monomers for every FVE monomer in the copolymer, then such a copolymer can flow on heating. If there are less than 30 TFE monomers per FVE monomer, such a copolymer is amorphous and does flow on heating.

The thermostability of the synthesized copolymer and PTFE as tested by differential-thermal analysis are presented in Figure 6, Curve 2 and listed in Table III. The molecular flow of the copolymer con-

**TABLE II**  
Molecular and Topological Structures of Powders of Copolymer of FVE with TFE

| Analyzed parameters                          | Co-axial orientation of vectors |       | Perpendicular orientation of vectors |       |
|--|---------------------------------|-------|--------------------------------------|-------|
|  |                                 |       |                                      |       |
| Share of FVE in the copolymer, % mole        |                                 |       |                                      |       |
|  | 2.4                             | 3.5   | 2.4                                  | 3.5   |
| Amorphous region                             |                                 |       |                                      |       |
| $T_g, ^\circ\text{C}$                        | -7                              | -10   | 2                                    | -4    |
| $\alpha_1 \cdot 10^5 \text{ deg}^{-1}$       | 10.9                            | 11.5  | 13.1                                 | 12.6  |
| $\alpha_2 \cdot 10^5 \text{ deg}^{-1}$       | 31.5                            | 26.4  | 49.4                                 | 35.1  |
| $V_f$  | 0.164                           | 0.118 | 0.299                                | 0.182 |
| $\overline{M}_{gn} \cdot 10^{-3}$            | 35.4                            | 10.9  | 754.9                                | 204.0 |
| $\overline{M}_{gw} \cdot 10^{-3}$            | 64.8                            | 19.1  | 1207.8                               | 310.0 |
| $K_a$  | 1.83                            | 1.75  | 1.60                                 | 1.52  |
| $\phi_a$                                     | 0.65                            | 0.69  | 0.83                                 | 0.75  |
| Crystalline portion                          |                                 |       |                                      |       |
| $T_m, ^\circ\text{C}$                        | 290                             | 160   |                                      |       |
| $\alpha_k \cdot 10^5 \text{ deg}^{-1}$       | 205.6                           |       |                                      |       |
| $\overline{M}_n^{cr1} \cdot 10^{-3}$         | 31.6                            | 398.1 |                                      |       |
| $\phi_{cr}$                                  | 0.35                            | 0.11  | 0.00                                 | 0.00  |
| High-temperature amorphous (cluster) region  |                                 |       |                                      |       |
| $T_{cl}, ^\circ\text{C}$                     |                                 | 200   | 280                                  | 195   |
| $\alpha'_{cl} \cdot 10^5 \text{ deg}^{-1}$   |                                 | 26.3  | 49.8                                 | 35.3  |
| $M_{(n)cl} \approx M_{(w)cl} \times 10^{-3}$ |                                 | 7.1   | 6.3                                  | 4.5   |
| $K_{cl}$                                     |                                 | 1     | 1                                    | 1     |
| $\phi_{cl}$                                  | 0.00                            | 0.2   | 0.17                                 | 0.25  |
| $T_f, ^\circ\text{C}$                        | 325                             | 215   | 295                                  | 207   |
| Values averaged between regions              |                                 |       |                                      |       |
| $\overline{M}_w \cdot 10^{-3}$               | 53.2                            | 58.4  | 1003.6                               | 233.6 |
| $K_{an}$                                     | 0.35                            | 0.11  |                                      |       |

taining 2.4 mol % of FVE occurs after melting of its low melting crystalline portion, i.e., after  $T_f = 325^\circ\text{C}$ . The DTA curve shows that the copolymer is amorphous-crystalline up to  $285^\circ\text{C}$  (Fig. 6, Curve 2). The endothermic melting of the crystalline portion ends at  $\sim 415^\circ\text{C}$ , when the copolymer becomes completely amorphous. Thermal degradation of the copolymer macromolecules begins above  $440^\circ\text{C}$ . A loss of mass occurs as the polymers begin to decompose, as shown by thermogravimetric analysis of the copolymer (Fig. 5, Curve 5). As seen from the TGA and TMS curves, the temperature at which mass loss begins ( $440^\circ\text{C}$ ) is  $115^\circ\text{C}$  higher than the temperature of molecular flow of the copolymer ( $T_f = 325^\circ\text{C}$ ). Thus, such a copolymer has thermostability similar to that of PTFE. However, increasing the FVE content in the copolymer composition causes more defects in its crystalline structure and decreases the thermostability. Therefore, on the curve of DTA of copolymers containing 3.5 mol % of FVE, a precise temperature of flow is not observed. So, for the production of a fusible and thermostable copolymer of FVE with TFE, the FVE content in this copolymer cannot be more than 2.4 mol %. This amount of FVE as a comonomer is much less than the amount of the comonomer HFP needed for production a fusible and thermostable copolymer with TFE.<sup>6</sup>



**TABLE III**  
The Data of the Differential-Thermal Analysis of PTFE and the Copolymer of TFE with FVE

| FVE content<br>in copolymer | Temperature of % weight loss |     |      | $T_m$ , °C <sup>a</sup> | Analysis conditions  |
|-----------------------------|------------------------------|-----|------|-------------------------|----------------------|
|                             | -0%                          | -5% | -50% |                         |                      |
| Mol %                       | $T$ , °C                     |     |      |                         |                      |
| 0.71                        | 460                          | 512 | 572  | 315                     | Ni crucible, He      |
| 1.39                        | 450                          | 510 | 570  | 315                     | ceramic crucible, He |
| 1.92                        | 445                          | 500 | 562  | 312                     | ceramic crucible, He |
| 2.40                        | 435                          | 490 | 558  | 310                     | ceramic crucible, He |
| 3.50                        | 410                          | 470 | 510  | -                       | ceramic crucible, He |
| 3.50                        | 415                          | 473 | 510  | -                       | Ni crucible, He      |
| 0.0                         | 470                          | 526 | 590  | 327                     | Ni crucible, He      |

<sup>a</sup> The temperature of melting is determined by differential-thermal analysis.

The high thermostability and stability to atmospheric influences allows for the production of the FVE copolymer with TFE without using additional thermo- and photostabilizers. Tests show that the mechanical and dielectric properties, as well as the chemical properties and thermostability of the copolymers of TFE with FVE are similar to those of PTFE. In addition, the FVE can be synthesized using industrial waste from TFE production. The low molecular flow temperature of the copolymer containing 2.4 mol % of FVE begins of 325°C and coupled with the degradation temperature of 440°C will allow the processing of this copolymer using the typical industrial methods used to process thermoplastics. The parameters of breaking load (28.1 MPa) and the rupture elongation (433%) of FVE/TFE copolymers ((2.4 mol % of FVE) are comparable with parameters (27.4 MPa, 405%) of synthesized PTFE. The fluidity of the copolymer is 4.8 g during 10 min at 297°C and under a cargo of 5 kg. Thus, the use of FVE as a comonomer for copolymerization with TFE is better than the use of HFP as the comonomer.

The synthesized copolymer behaves in the same way under  $\gamma$ -irradiation as PTFE. The molecular relaxation characteristics of synthesized PTFE and FVE irradiated by  $\gamma$ -rays are listed in Table IV. The TMC of irradiated PTFE shows a completely amorphous topological structure consisting of amorphous and cluster portions (Table IV), instead of the amorphous-crystalline structure of virgin PTFE (Table I). The nature of the changes in the block structure of PTFE and the development of amorphous structure on  $\gamma$ -irradiation has been discussed in detail.<sup>14,33,34</sup> The  $\gamma$ -irradiation of the FVE/TFE copolymer (2.4 mol % of FVE) leads to the disappearance of the crystal portions the TMC of the irradiated copolymer show only amorphous and cluster regions (Table IV), essentially the same result as for pure

PTFE. Thus,  $\gamma$ -irradiation increases the degree of amorphous material and reduces the temperature of melting. However, the changes due to radiation could be quite different.  $\gamma$ -irradiation of the PTFE macromolecule<sup>14,33,34</sup> leads to loss of a fluorine atom by breaking a C-F bond which leads to loss of crystallinity and, consequently, mechanical durability of the polymer. The larger volume of the  $-\text{OCF}_2\text{CF}_2\text{Cl}$  functional group in FVE/TFE copolymers will break up the helical conformation of virgin PTFE chains which should affect the radiolysis and change the chemistry. This will be pursued in future work.

**TABLE IV**  
Molecular and Topological Structures of the Irradiated PTFE and FVE Samples Registered in Coaxial Orientation of Vectors<sup>a</sup>

| Parameters                                  | PTFE  | FVE/TFE |
|---|-------|---------|
| Amorphous region                            |       |         |
| $T_{gr}$ , °C                               | 16    | -12     |
| $\alpha_1 \cdot 10^5 \text{ deg}^{-1}$      | 8.25  | 9.4     |
| $\alpha_2 \cdot 10^5 \text{ deg}^{-1}$      | 39.23 | 24.5    |
| $V_f$                                       | 0.272 | 0.118   |
| $\bar{M}_{gn} \cdot 10^{-3}$                | 463.0 | 120     |
| $\bar{M}_{gw} \cdot 10^{-3}$                | 910.0 | 191     |
| $K_a$                                       | 1.96  | 1.59    |
| $\phi_a$                                    | 0.80  | 0.88    |
| High-temperature amorphous (cluster) region |       |         |
| $T_{cl}$ , °C                               | 337   | 89      |
| $\alpha_{cl} \times 10^5 \text{ deg}^{-1}$  | 40.33 | 40.3    |
| $(M_{n(cl)} \times 10^{-6})$                | 0.089 | 79.1    |
| $(M_{w(cl)} \times 10^{-6})$                | 0.114 | 79.1    |
| $K_{cl}$                                    | 1.28  | 1       |
| $\phi_{cl}$                                 | 0.2   | 0.12    |
| Values averaged between regions             |       |         |
| $T_f$ , °C                                  | 371   | 198     |
| $\bar{M}_w \cdot 10^{-6}$                   | 0.729 | 0.1776  |

<sup>a</sup> There is 2.4 mol % FVE share in FVE/TFE. Dose of irradiation by  $\gamma$ -rays of <sup>60</sup>Co at 27°C is 140 kGy.



copolymer has a completely amorphous di-block morphology. Only small amounts of FVE (1.0-2.4 mol %) provide high thermostability and a decrease of the fusion temperature of the copolymer. Such a copolymer is a thermoplastic analogue of PTFE as it can be processed by methods widely used for processing the majority of industrial thermoplastics.

## References

1. Ebnesajjad, S.; Khaladkar, P. R. *Fluoropolymer Applications in the Chemical Processing Industries: The Definitive User's Guide and Databook*; William Andrew Publishing/Plastics Design Library: Norwich, New York, 2005.
2. Ebnesajjad, S. *Fluoroplastics: Melt Processible Fluoropolymers: The Definitive Users Guide and Databook*; William Andrew Publishing/Plastics Design Library: Norwich, New York, 2002.
3. Ebnesajjad, S. *Fluoroplastics: Non-melt Processible Fluoroplastics*; William Andrew Publishing/Plastics Design Library: Norwich, New York, 2000.
4. Améduri, B.; Boutevin, B. *Well-Architected Fluoropolymers: Synthesis, Properties and Applications*; Elsevier: Amsterdam, 2004.
5. Schiers, J., Ed. *Modern Fluoropolymers: High Performance Polymers for Diverse Applications (Wiley Series in Polymer Science)*; Wiley: New York, 1997.
6. Panshin, J. A.; Malkevich, S. G. *Dunaevskaja, S. Ftoroplasti (Fluoroplastics)*; Khimiya: Leningrad, 1978.
7. Kochkina, L. G.; Erohova, V. A.; Loginova, N. N. *Z. Prikladnoi Khymii (Russ. J. Appl. Chem.)* 1984, 1126.
8. Sokolov, S. V.; Sass, V. P. Z. *Vsesouyuznogo Khimicheskogo Obshestvo imeni D.I. Mendeleeva (J. D. I. Mendeleev All-Unin Chem. Soc.)* 1981, 26, 303.
9. Alfrey, T., Jr.; Price, C. C. *J Polym Sci* 1947, 2, 101.
10. Skobina, A.; Volkova, E.; *Radiazionnaya Khimiya Polimerov (Radiation Chemistry of Polymers)*; Nauka: Moscow, 1966.
11. Allayarov, S. R.; Kim, I. P.; Barkalov, I. M.; Ilín, A. N. *Vysokomol. Soedin A* 1990, 32, 761.
12. Scherer, K. V.; Ono, T.; Yamanouchi, K.; Fernandez, R. E.; Henderson, P.; Goldwhite, H. *J Am Chem Soc* 1985, 107, 718.
13. Olkhov, Y. A.; Allayarov, S. R.; Konovalova, T. A.; Kispert, L. D.; Nikles, D. E. *J Appl Polym Sci* 2008, 108, 2085.
14. Olkhov, Y. A.; Allayarov, S. R.; Chernyshova, T. E.; Barkalov, I. M.; Kispert, L. D.; Thrasher, J. S.; Fernandez, R. E.; Nikles, D. E. *High Energy Chem* 2006, 40, 310.
15. Evreinov, V. V.; Tkachuk, Y. G.; Entelis, S. G. *Vysokomol Soedin A* 1973, 15, 4.
16. Brice, T. J.; Severson, W. A. *US Patent* 2,790,815, 1957.
17. Vorovich, I. I.; Ustinov, Iu. A. *J Appl Math Mech* 1959, 23, 637.
18. Olkhov, Y. A.; Allayarov, S. R.; Tolstopyatov, E. M.; Grakovich, P. N.; Kalinin, L. A.; Dobrovol'skii, Y. A.; Dixon, D. A. *High Energy Chem* 2010, 44, 63.
19. Olkhov, Y. A.; Allayarov, S. R.; Kochetkova, G. V. *Soedineniya ftora, Khimiya, Tekhnologiya, Primenenie. (Compounds of Fluorine, Chemistry, Technology, Application)*; Teza: St. Petersburg, 2009.
20. Olkhov, Y. A.; Baturin, S. M.; Irzhak, V. I. *Vysokomol Soedin A* 1996, 38, 849.
21. Jurkowski, B.; Olkhov, Y. A. *Thermochim Acta* 2004, 414, 85.
22. Olkhov, Y. A.; Jurkowski B. *J Appl Polym Sci* 1997, 65, 499.
23. Olkhov, Y. A.; Jurkowski, B.; Pesetskii, S. S.; Krivoguz, M.; Kelar, K. *J Appl Polym Sci* 1999, 71, 1771.
24. Jurkowska, B.; Olkhov, Y. A.; Jurkowski, B. *J Appl Polym Sci* 1998, 68, 2159.
25. Jurkowski, B.; Olkhov, Y. A. *Thermochim Acta* 2004, 414, 243.
26. Olkhov, Y. A.; Allayarov, S. R.; Nikolskii, V. G.; Dixon, D. A. *Khimiya Vysokikh Energii* 2011, 45, 40.
27. Barb, W. G. *J Polym Sci* 1953, 11, 117.
28. Mayo, F. R.; Lewis, F. M. *J Am Chem Soc* 1944, 66, 1594.
29. Gal'perin, E. L.; Tsvankin, D. *J Vysokomol. Soedin A* 1976, 18, 2691.
30. Olkhov, J. A.; Irzhak, V. I.; Baturin, S. M. *RF Patent* 2,023,255, 1994.
31. Wall, L. A. *Fluoropolymers*; Wiley Interscience: New York, 1972.
32. Simha, R.; Boyer, R. F. *J Chem Phys* 1962, 37, 1003.
33. Allayarov, S. R.; Konovalikhin, S. V.; Olkhov, Y. A.; Jackson, V. E.; Kispert, L. D.; Dixon, D. A.; Ila, D.; Lappan, U. *J Fluor Chem* 2007, 128, 575.
34. Allayarov, S. R.; Gordon, D. A.; Kim, I. P. *J Fluor Chem* 1999, 96, 61.